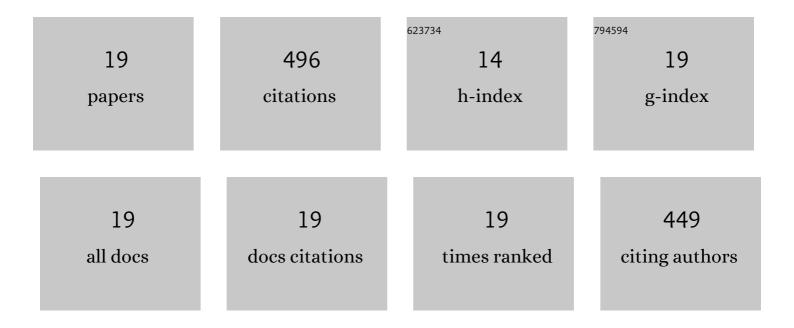
Caitlin M A Mcqueen

List of Publications by Year in descending order

Source: https://exaly.com/author-pdf/7592600/publications.pdf Version: 2024-02-01



#	Article	IF	CITATIONS
1	Comparative chemical investigations of alum treated archaeological wood from various museum collections. Heritage Science, 2021, 9, .	2.3	4
2	Oxidative degradation of archaeological wood and the effect of alum, iron and calcium salts. Heritage Science, 2020, 8, .	2.3	2
3	Isoselenocarbonyl complexes. Dalton Transactions, 2019, 48, 2000-2012.	3.3	16
4	Selective formylation or methylation of amines using carbon dioxide catalysed by a rhodium perimidine-based NHC complex. Green Chemistry, 2019, 21, 538-549.	9.0	65
5	Ammonium alum in alum-treated wooden artefacts: discovery, origins and consequences. Heritage Science, 2019, 7, .	2.3	6
6	Climatically Induced Degradation Processes in Conserved Archaeological Wood Studied by Time-lapse Photography. Studies in Conservation, 2019, 64, 115-123.	1.1	6
7	Identification of inorganic compounds in composite alum-treated wooden artefacts from the Oseberg collection. Scientific Reports, 2018, 8, 2901.	3.3	14
8	Iridium complexes of perimidine-based N-heterocyclic carbene pincer ligands <i>via</i> aminal C–H activation. Dalton Transactions, 2018, 47, 1577-1587.	3.3	22
9	Controlled depolymerisation assessed by analytical ultracentrifugation of low molecular weight chitosan for use in archaeological conservation. European Biophysics Journal, 2018, 47, 769-775.	2.2	16
10	Temperature- and humidity-induced changes in alum-treated wood: a qualitative X-ray diffraction study. Heritage Science, 2018, 6, .	2.3	6
11	Navigating conservation strategies: linking material research on alum-treated wood from the Oseberg collection to conservation decisions. Heritage Science, 2018, 6, .	2.3	21
12	Chemical analyses of extremely degraded wood using analytical pyrolysis and inductively coupled plasma atomic emission spectroscopy. Microchemical Journal, 2016, 124, 368-379.	4.5	42
13	Ruthenium and osmium complexes of dihydroperimidine-based N-heterocyclic carbene pincer ligands. Dalton Transactions, 2015, 44, 20376-20385.	3.3	26
14	Arrested B–H Activation en Route to Installation of a PBP Pincer Ligand on Ruthenium and Osmium. Organometallics, 2014, 33, 1977-1985.	2.3	46
15	Dihydroperimidine-Derived PNP Pincer Complexes as Intermediates en Route to N-Heterocyclic Carbene Pincer Complexes. Organometallics, 2014, 33, 1909-1912.	2.3	30
16	Novel Carbon Monochalcogenide Coordination Mode: [Rh2{μ-SeCMo(CO)2(Tp*)}2(η4-cod)2] (Tp* =) Tj ETQqO 2482-2485.	0 0 rgBT / 2.3	Overlock 10 28
17	Dihydroperimidine-Derived N-Heterocyclic Pincer Carbene Complexes via Double C–H Activation. Organometallics, 2012, 31, 8051-8054.	2.3	67

Alkynyl Selenolate Complexes of Iron, Nickel, and Molybdenum. Organometallics, 2010, 29, 6350-6358. 2.3 15

#	Article	IF	CITATIONS
19	Iridiumâ^'Molybdenum Carbido Complex via Câ^'Se Activation of a Selenocarbonyl Ligand: (μ-Se ₂)[Ir ₂ {C≡Mo(CO) ₂ (Tp*)} ₂ (CO) ₂ (P (Tp* = hydrotris(dimethylpyrazolyl)borate). Organometallics, 2009, 28, 6639-6641.	Ph< sub >	3a